An Analysis of Deep Drawing Process in the Punchless Drawing Utilizing Lateral Fluid Pressure

An Analysis of Deep Drawing Process in the Punchless Drawing Utilizing Lateral Fluid Pressure

Kenji ASAKURA*, Nobuo KOBAYASHI*, Masahide KOHZU* and Nobuyuki SUZUKI**

(Received June 15, 1983)

A numerical analysis has been made to confirm the tool condition of this new punchless drawing clarified experimentally in previous paper. By the simulation of deformation process using matrix method, the C.S.P. curves representing calculated shell profiles at progressive drawing stages were obtained. The deformation behavior of blank and its contact behavior on die shoulder under various tool conditions were analyzed, and it was found that the optimum die radius for this punchless drawing can be presumed theoretically.

1. Introduction

The authors[1] have already clarified experimentally the drawing characteristics in the deep drawing utilizing lateral fluid pressure and have proposed its punchless drawing. The punchless drawing became feasible for 0.8 mm-thick, 60 mm-diam soft aluminum blanks by using the die having a die radius of 3.0 mm. The purpose of this study is to confirm this optimum die radius by the simulation of deformation process using matrix method.

2. Analysis

An analysis of deep drawing process by matrix method had been reported by Tatenami, Nakamura and Saito[2)~6)]. The matrix method[4)] considering the bending and unbending of blank on die shoulder and the contact of blank with punch and die was applied to this study.

In this method, a circular blank is divided into n_a annular elements called "major elements" as shown in Fig. 1. Moreover, each major element is also divided into n_e stratiform elements called "minor elements".

In this formulation, some assumptions are used; (1) Kirchhoff-Love's hypothesis is adopted, so shearing deformation is neglected. (2) There is no flexural rigidity of each minor element. (3) There is no change in curvature in the meridian direction on each element.

The moment acting on a major element are derived from stress components of its minor elements. The judgement on the contact of blank with tools is made for each major element.

Vertical, meridian and moment equilibrium equations of a major element i and the equations of meridian normal force and moment acting on the boder $i+1$ make

* Department of Metallurgical Engineering, College of Engineering.
** Japan Aircraft Co., Ltd.

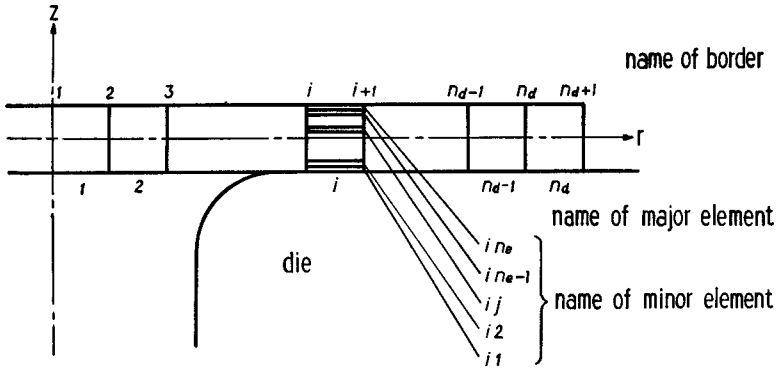

Fig. 1 Division of blank into elements.

the equation of five rows,

$$C_{1i}\{\dot{X}\}_i+C_{2i}\begin{Bmatrix}\dot{N}_i\\ \dot{N}_{i+1}\end{Bmatrix}+C_{3i}\begin{Bmatrix}\dot{M}_i\\ \dot{M}_{i+1}\end{Bmatrix}+C_{4i}\begin{Bmatrix}\dot{Q}_i\\ \dot{Q}_{i+1}\end{Bmatrix}+C_{5i}\dot{P}_i=0\,, \tag{1}$$

where $\{\dot{X}\}_i$ is the variable column vector composed of the increments of lean angles $\dot{\varphi}_i$, $\dot{\varphi}_{i+1}$ and the increments of position components $\dot{r}_i$, $\dot{z}_i$, $\dot{r}_{i+1}$, $\dot{z}_{i+1}$ of both boders i, $i+1$ of the major element i. $\dot{N}_i$, $\dot{M}_i$ and $\dot{Q}_i$ are the increments of meridian normal force, moment and shearing force acting on the boder i, respectively. And $\dot{P}_i$ is the contact force between tool and the major element i.

The compatibility equation of displacement on the border of major element is shown as

$$C_{6i}\{\dot{X}\}_i=0\,. \tag{2}$$

Unknown variables remained finaly are $(7n_d+3)$. About all elements, there are $(6n_d-2)$ rows in equations (1), (2). There are (n_d+5) boundary conditions described as follows. The geometical boundary conditions are $\dot{r}_1=0$, $\dot{\varphi}_1=0$ at the center and the boundary conditions on force are $\dot{Q}_{nd+1}=0$, $\dot{N}_{nd+1}=0$, $\dot{M}_{nd+1}=0$ at the rim. About each of n_d major elements, if the element is in contact with tool, a geometical boundary condition so as to keep the element in contact is used. And if the element is off tool, a boundary condition on force $\dot{P}_i=0$ is used. By use of these boundary conditions and the increment of punch stroke for the deformation parameter, the simultaneous linear equations are solved.

When applying this matrix method[4] to the punchless drawing utilizing lateral fluid pressure, the increment of displacement of rim of flange was used as the deformation parameter in place of the increment of punch stroke. In the punchless drawing, as shown in Fig. 2, the hold-down cylinder corresponding to blank holder has a protrusion to seal the pressurized oil and the protrusion penetrates the blank slightly at the inner part of the flange. On calculation, a simplification was introduced by assuming that the bottom of hold-down cylinder is flat. This simplification may be allowed as the deformation process of blank on die shoulder is not hardly affected by the deformation of flange.

Dividing the blank into elements, the fine division is advantageous in accuracy

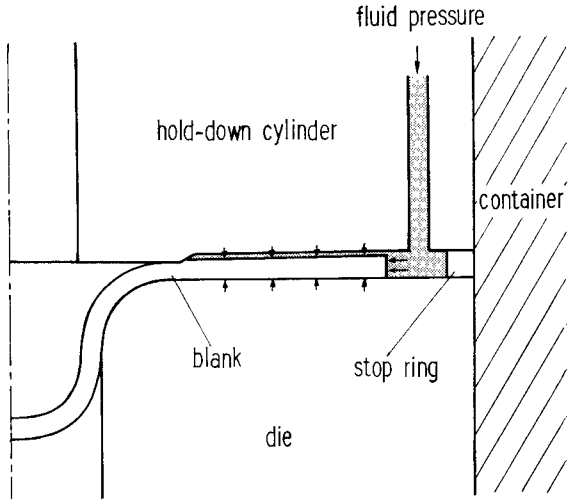

Fig. 2 Schematic diagram of main equipment used for punchless drawing utilizing lateral fluid pressure.

of calculation, but is disadvantageous in computational time. So, the blank radius of 17.88 mm, which is smaller than the practical blank radius of 30 mm used in experiment[1], was adopted to calculate accurately in short time. This blank radius may be sufficient to simulate the deformation process of blank on die shoulder.

About major elements, three ranges of 0~4 mm, 4~7 mm and 7~17.88 mm in distance from axis were divided into 2, 3 and 34 equal length parts, respectively. Such coarse division in inner range may be allowed as the deformation in its range is far smaller than that in outer range. And each major element was also divided into 5 equal stratiform minor elements.

The calculation was carried out using the material constants of soft aluminum sheet (0.8 mm in thick), of Young's modulus 70 GPa, the Poison ratio 0.33, the yield stress 60 MPa, and work hardening coefficient 150 MPa. The die throat diameter $2r_d$ was 16.9 mm, and the radii of die profiles ρ_d were 1.0, 2.5, 3.0 and 4.0 mm.

3. Results

By the simulation of deformation process using matrix method, the deformation behavior of blank and its contact behavior on die shoulder were analyzed.

3.1 C.S.P. curve

Figure 3 shows the comparison of practical shell profile with calculated shell profile. In this figure, solid lines show the cross sections of the practical shells obtained at various drawing stages in the punchless drawing with die having the optimum die radius, ρ_d=3.0 mm[1]. And alternate long and short dash lines show the curves representing calculated shell profiles, hereinafter called C.S.P. curves, for the same drawing stages. The C.S.P. curve is described by connecting the centers of borders of all major elements. Considering the thickness of blank for the C.S.P.

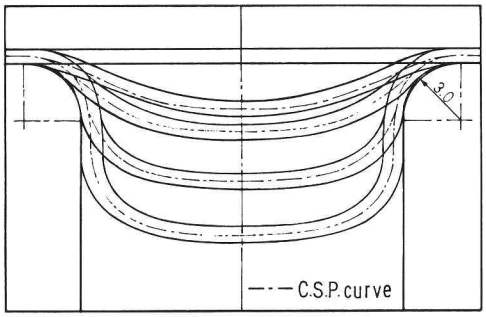

Fig. 3 Comparison of practical shell profile with calculated shell profile.

curve, the calculated shell profile can be described.

In this figure, the C.S.P. curve correspondes to the center line of the practical shell profile at each drawing stage. From this result, it is found that the drawing process under the optimum tool condition, under which the deformation of blank is axisymmetrical, is represented with high fidelity by the group of these C.S.P. curves.

3.2 Deformation behavior of blank on die shoulder

Figure 4 shows the shape of cups drawn in the punchless drawing with three dies having different die radii[1]. For the optimum die radius, ρ_d=3.0 mm, the cup has perfectly cylindrical wall as shown in Fig. 4(b). For smaller die radius, ρ_d=1.0 mm, the cup is hollowed at four portions of its wall by buckling as shown in Fig. 4(a). And, for larger die radius, ρ_d=4.0 mm, the cup is wrinkled at the part bended on die shoulder as shown in Fig. 4(c). For die radius ρ_d of 2.5 mm which is slightly smaller than the optimum die radius, the cup had perfectly cylindrical wall in most caces but rarely it was hollowed at its wall by buckling.

Figure 5 (a)~(d) show the C.S.P. curves at progressive drawing stages during the process of punchless drawing with dies having die radii ρ_d of 1.0, 2.5, 3.0 and 4.0 mm, respectively. Fig. 6 (a)~(d) show the C.S.P. curves at progressive drawing stages during the process of punchless drawing with the assumed dies obtained by removing the shoulders of the original dies. Fig. 6 represents the deformation behavior of blank throughout the drawing process in which the blank is not restrained by die shoulder. In these figures, the depth of drawing S corresponding to z co-

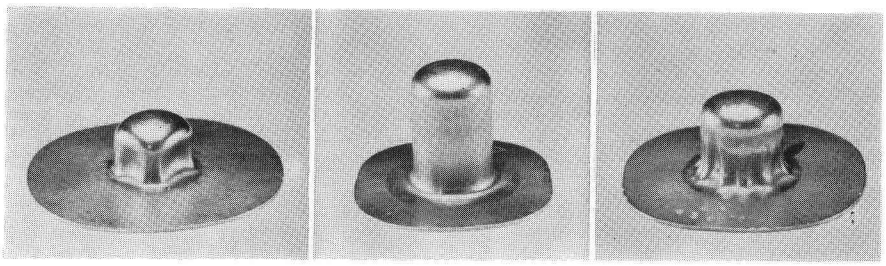

	(a)	(b)	(c)
ρ_d:	1.0 mm	3.0 mm	4.0 mm

Fig. 4 Shape of cups drawn with dies having various die radii ρ_d.

ordinate of center of blank is taken as ordinate and the distance from axis of die hole to center of the border of major element is taken as abscissa. And, the curves representing die hole contours are describe with a larger radii than practical die radii

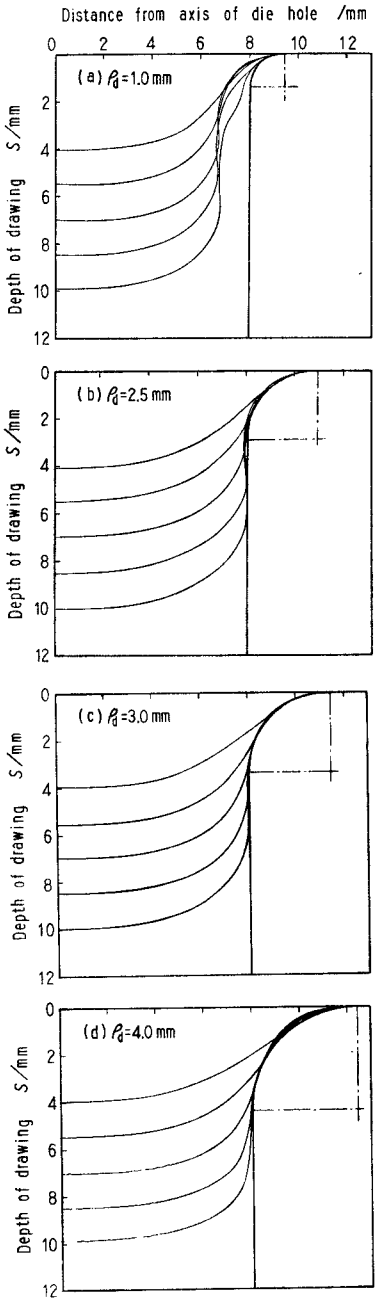

Fig. 5 C.S.P. curves at progressive drawing stages during process of punchless drawing.

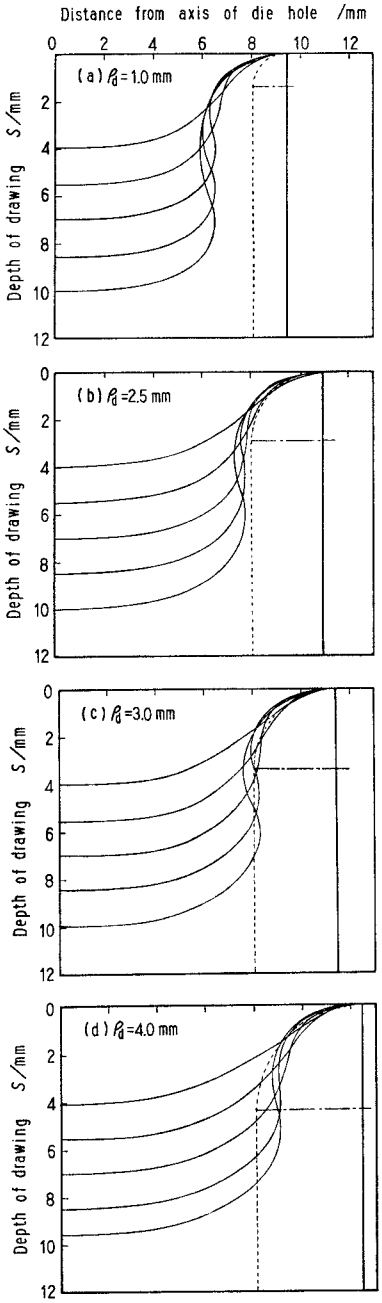

Fig. 6 C.S.P. curves at progressive drawing stages during process of punchless drawing with assumed die.

by a half of initial thickness of blank.

For die radius ρ_d of 1.0 mm, the C.S.P. curves are far apart from the curve representing die hole contour as shown in Fig. 5(a), and the same result is obtained for the assumed die as shown in Fig. 6(a).

For the optimum die radius, ρ_d=3.0 mm, as shown in Fig. 5(c), the C.S.P. curves are scarcely apart from the curve representing die hole contour at the drawing stages at which the cup wall is formed. For ρ_d=2.5 mm and ρ_d=4.0 mm, as shown in Fig. 5(b) and (d), the C.S.P. curves are slightly apart from the curves representing die hole contours at the range from the central part of die shoulder to its exit and at the middle part of die shoulder, respectively. Therefore, it is recognized that the group of C.S.P. curves obtained for the optimum die radius, ρ_d=3.0 mm, represents the deformation process of blank fitting best on die shoulder.

Three groups of C.S.P. curves for the assumed dies shown in Fig. 6(b)~(d) differ in the distance from each curve representing die hole contour of the original die shown by dotted line. But superposing the curves representing die hole contours of the assumed dies shown by solid lines in these figures, every groups of C.S.P. curves overlaps at several points with the curve representing die hole contour of the optimum die.

3.3 Variation of contact positions between blank and die shoulder

Figure 7(a)~(c) show the variation of contact positions between blank and die shoulder in the processes of punchless drawing with dies having die radii ρ_d of 2.5, 3.0 and 4.0 mm, respectively. In these figures, the depth of drawing S is taken as abscissa and the contact position represented by central angle φ measured from the entrance of die to a contact point on die shoulder is taken as ordinate.

In these figures, the contact positions vary with increasing depth of drawing and they can be classified into two groups. One of these groups is located at the neighborhood of the entrance of die (φ=0~15 deg.) and the other is located at the range from the central part of die shoulder to its exit (φ=90 deg.).

For die radius ρ_d of 2.5 mm, as shown in Fig. 7(a), the blank is in partial contact with die shoulder at the neighborhood of the entrance of die throughout the drawing process. And the variation of contact position in the range from the central part of die shoulder to its exit is as follows. When depth of drawing S reaches to 5.5 mm, the blank comes in contact with die shoulder at the position of φ=65 deg. And then, the contact position shifts toward the exit of die with increasing depth of drawing and it reaches there at depth of drawing S of 7 mm. And in the following process, in which the cup wall is formed, the blank is out of contact with die shoulder for a while, but it comes in contact again at the position of φ=35 deg. at depth of drawing S of 9 mm.

For the optimum die radius, ρ_d=3.0 mm, as shown in Fig. 7(b), the blank is in partial contact with die shoulder at the neighborhood of the entrance of die throughout the drawing process. And the variation of contact positions in the range from the central part of die shoulder to its exit is as follows. When depth of drawing S reaches to 4.5 mm, the blank comes in contact with die shoulder at the position of φ=50 deg. And then, the contact position shifts toward the exit of die with in-

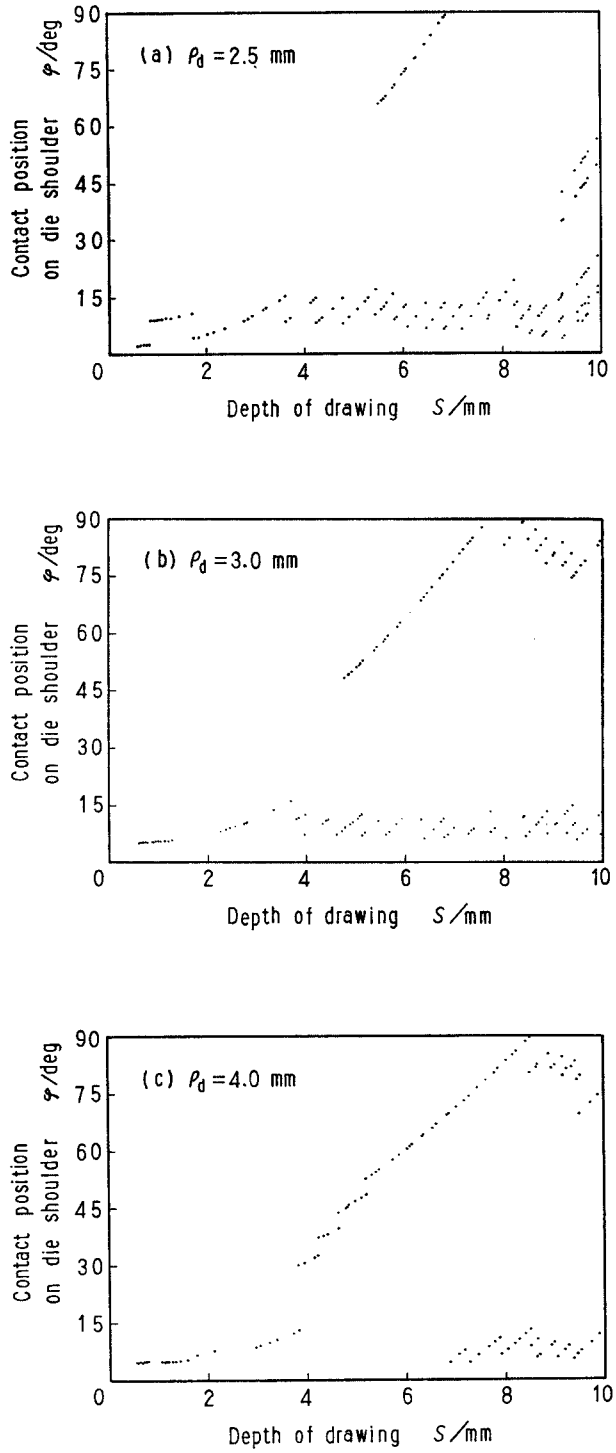

Fig. 7 Variation of contact positions between blank and die shoulder in drawing process.

creasing depth of drawing and it reaches there at depth of drawing S of 7.5 mm. And, throughout the following process, in which the cup wall is formed, the blank is always in contact with die shoulder at the neighborhood of its exit.

For die radius ρ_d of 4.0 mm, as shown in Fig. 7(c), the blank is out of contact with die shoulder at the neighborhood of the entrance of die for depth of drawing in range from 4 to 7 mm. And the variation of contact positions in the range from the central part of die shoulder to its exit is as follows. When depth of drawing S reaches to 4 mm, the blank comes in contact with die shoulder at the position of $\varphi=30$ deg. And then, the contact position shifts toward the exit of die with increasing depth of drawing and it reaches there at depth of drawing S of 8.5 mm. And, throughout the following process, in which the cup wall is formed, the blank is always in contact with die shoulder at the neighborhood of its exit in the same manner as the cace of the optimum die radius, $\rho_d=3.0$ mm.

4. Consideration

In the preceding chapter, the deformation behavior of blank on die shoulder and the variation of its contact position were analyzed by the simulation using matrix method. Based on these results, the practical deformation behavior of blank in punchless drawing (see Fig. 4) are considered as follows.

For die radius ρ_d of 1.0 mm, the C.S.P. curves were far apart from the curve representing die hole contour. Therefore the blank was quite unrestrained by die shoulder. So, it is consideres that the buckling of blank was occured by circumferential stress at the portion where the curvature of blank was reduced by unbending.

For die radius ρ_d of 2.5 mm, the C.S.P. curves were slightly apart from the curve representing die hole contour. And the blank was unrestrained by die at the neighborhood of its exit in the process in which the cup wall was formed. On the other hand, for the optimum die radius, $\rho_d=3.0$ mm, the blank was restrained there throughout that process. Therefore, it is considered that hollows on the cup drawn with die having die radius ρ_d of 2.5 mm were caused by the unrestraint at the neighborhood of exit of die where the curvature of blank is reduced by unbending.

For die radius ρ_d of 4.0 mm, the C.S.P. curves were slightly apart from the curve representing die hole contour. And the blank was unrestrained by die except for the neighborhood of its entrance and exit in the same manner as the cace of the optimum die radius, $\rho_d=3.0$ mm. However, this die radius itself was larger than the optimum die radius, so the blank being drawn with this die had smaller curvature, wider unrestrained region on die shoulder and larger quantity of the drawing deformation in that region than the blank being drawn with the optimum die. Therefore, it is considered that wrinkles on the cup drawn with die having die radius ρ_d of 4.0 mm were caused by these factors.

From above, the considerable points to draw a blank without buckling in the punchless drawing and to obtain the cup having perfectly cylindrical wall are briefed as follows. The die radius must have the sufficient size to keep the contact of blank with die shoulder at the neighborhood of its exit and must be minimized to avoid the occurrence of wrinkles.

When general working condition, as the material and size of cup, are given, the optimum die radius for the punchless drawing utilizing lateral fluid pressure can be presumed in the following way. Any die radius is at first decided provisionally, and then the C.S.P. curves for the assumed die obtained by removing the die shoulder of the provisional die are described. And, from the mean process of drawing deformation represented by the group of those C.S.P. curves, the approximate value of the optimum die radius is determined.

5. Conclusion

In this study, the deformation behavior of blank and its contact behavior on die shoulder in this punchless drawing clarified experimentally in previous paper were analyzed by the simulation of deformation process using matrix method, and its optimum die radius obtained in experiment was confirmed theoretically.

The results obtained may be summarized as follows.

(1) The deep drawing process under the optimum tool condition is represented with high fidelity by the group of the C.S.P. curves, which represent calculated shell profiles.

(2) The group of C.S.P. curves obtained for the optimum die radius, ρ_d=3.0 mm, represents the deformation process of blank fitting best on die shoulder.

(3) For the assumed dies obtained by removing the shoulders of original dies, every groups of C.S.P. curves overlap at several point with the curve representing die hole contour of the optimum die.

(4) The hollows on cup drawn with die having smaller die radius than the optimum value are caused by the unrestraint at the neighborhood of exit of die where the curvature of blank is reduced by unbending.

(5) The wrinkles on the cup drawn with die having larger die radius than the optimum value are caused by smaller curvature of blank, wider unrestrained region and larger drawing deformation on die shoulder.

(6) The optimum die radius for the punchless drawing can be presumed by the simulation of deformation process using the matrix method.

Acknowledgement

The authors wish to thank Professor K. Saito, Dr. T. Tatenami and Dr. Y. Nakamura of Osaka Industrial University for their helpful advice on the numerical solution.

References

1) K. Asakura, N. Kobayashi, T. Hanamoto and M. Kohzu, Bull. Univ. Osaka Prefecture, **31A**, 171 (1982).
2) T. Tatenami and K. Saito, Trans. JSME., **40**, 2537 (1974).
3) Y. Nakamura, T. Tatenami, T. Takagishi and K. Saito, J. Japan Soc. Tech. Plasticity, **19**, 772 (1978).
4) Y. Nakamura, T. Tatenami and K. Saito, ibid., **19**, 890 (1978).
5) Y. Nakamura, T. Tatenami and K. Saito, Numerical Methods in Industrial Forming Processes, Swansea, U.K., p. 677 (1982).
6) T. Tatenami, Y. Nakamura and K. Saito, ibid., p. 687 (1982).